

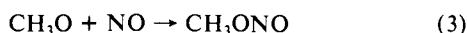
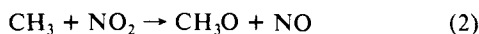
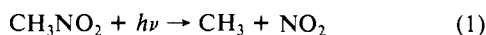
# Ab Initio Study of Rearrangements on the CH<sub>3</sub>NO<sub>2</sub> Potential Energy Surface

Michael L. McKee

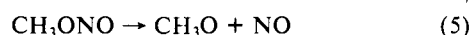
Contribution from the Department of Chemistry, Auburn University, Auburn, Alabama 36849.  
Received December 27, 1985

**Abstract:** A theoretical study has been performed for the thermal rearrangements connecting nitromethane, methyl nitrite, nitrosomethanol, and *aci*-nitromethane by using the 6-31G\* basis set to optimize geometries and introducing correlation at the MP2 level. The lowest calculated rearrangement pathways from nitromethane are to methyl nitrite ( $\Delta H^\ddagger = 73.5$  kcal/mol) and *aci*-nitromethane ( $\Delta H^\ddagger = 75.0$  kcal/mol). Nitrosomethanol, although predicted to be only 1.6 kcal/mol less stable, is separated by two high barriers from nitromethane. An elimination transition structure connecting methyl nitrite and formaldehyde plus nitroxyl is found to have an enthalpic barrier of 44.1 kcal/mol. Fragmentation reactions have enthalpies of reaction less than calculated barrier heights, suggesting that concerted rearrangements on the CH<sub>3</sub>NO<sub>2</sub> surface in general will not be observed.

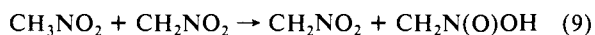
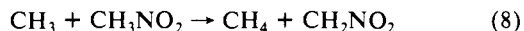
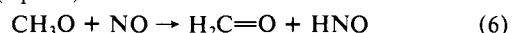
The photodecompositions of nitromethane<sup>1-9</sup> and methyl nitrite<sup>1,10-18</sup> have received considerable attention as model systems for studies in propellant ignition, combustion, and atmosphere pollution. Characterization of the above compounds and their decomposition products has included techniques such as microwave,<sup>16,19,20</sup> electron impact,<sup>21</sup> and NMR.<sup>22</sup> The threshold for photolysis of nitromethane is determined to be 86.6 kcal/mol (330 nm),<sup>1</sup> slightly higher than the threshold for methyl nitrite which is 77.3 kcal/mol (370 nm).<sup>1</sup> Identification of initial reaction products is difficult since any radicals produced may rapidly undergo secondary reactions. Photolysis of nitromethane can produce *cis*- and *trans*-CH<sub>3</sub>ONO as shown in eq 1-3 where reaction 2 is predicted to very rapid.<sup>23</sup>



The pyrolysis of nitromethane and methyl nitrite is generally regarded to occur by an initial bond rupture (eq 4 and 5).



Secondary reactions of these radicals can then account for a variety of products (eq 6-9).



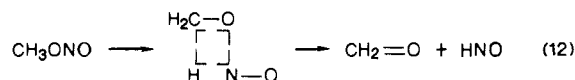
The known decomposition-recombination mechanism of nitromethane places a lower limit on the enthalpy of activation for the unimolecular rearrangement in eq 10 which must be higher



than the strength of a C-N bond (58.5 kcal/mol<sup>1</sup>) since this would be the enthalpy of activation for the formation of the radicals CH<sub>3</sub> and NO<sub>2</sub>. Similarly the barrier for eq 11 must be higher than



the strength of the central N-O bond which is found<sup>1</sup> to be 41.2 kcal/mol. The goal of this article is to provide an accurate description of the concerted thermal rearrangement barriers. While the initial step is generally acknowledged to be radical formation it is possible that the later observed products (or unobserved products) are due to unimolecular rearrangements. Indeed, a unimolecular elimination process has been proposed<sup>1</sup> involving a cyclic transition structure (eq 12).



In a related area, the reactions of the metal ion Co<sup>+</sup> with CH<sub>3</sub>NO<sub>2</sub> and CH<sub>3</sub>ONO have generated a rich field for chemical investigation.<sup>24</sup> Reaction pathways begin with the probable coordination of Co<sup>+</sup> to an oxygen followed by possible concerted rearrangement to a number of different products. It seems likely that the metal assists in the initial nitro-to-nitrite isomerization. If so, the concerted rearrangement surface in the absence of a metal ion would be valuable in interpreting results.

Previous theoretical calculations on nitromethane and methyl nitrite have been performed to study such aspects as the multi-configurational nature of the ground state,<sup>25-27</sup> the relative stability

(1) Batt, L.; Robinson, G. N. *The Chemistry of Amino, Nitroso, and Nitro Compounds and their Derivatives*; Patai, S., Ed.; Wiley: New York, 1982; Parts 1 and 2.

(2) Jacox, M. E. *J. Phys. Chem.* **1984**, *88*, 3373-3379.

(3) Jacox, M. E. *J. Phys. Chem.* **1983**, *87*, 3126-3135.

(4) Flicker, W. M.; Mosher, O. A.; Kuppermann, A. *J. Chem. Phys.* **1980**, *72*, 2788-2794.

(5) Blais, N. C. *J. Chem. Phys.* **1983**, *79*, 1723-1731.

(6) Schoen, P. E.; Marrone, M. J.; Schnur, J. M.; Goldbert, L. S. *Chem. Phys. Lett.* **1982**, *90*, 272-276.

(7) Kwok, H. S.; He, G. Z.; Sparks, R. K.; Lee, Y. T. *Int. J. Chem. Kinet.* **1981**, *13*, 1125-1131.

(8) Butler, L. J.; Krajnovich, D.; Lee, Y. T.; Ondrey, G.; Bersohn, R. *J. Chem. Phys.* **1983**, *79*, 1708-1722.

(9) Taylor, W. D.; Allston, T. D.; Moscato, M. J.; Fazekas, G. B.; Kozlowski, R.; Takacs, G. A. *Int. J. Chem. Kinet.* **1980**, *12*, 231-240.

(10) Jacox, M. E.; Rook, F. *J. Phys. Chem.* **1982**, *86*, 2899-2904.

(11) Müller, R. P.; Huber, J. R. *J. Phys. Chem.* **1983**, *87*, 2460-2462.

(12) Sanders, N.; Butler, J. E.; Pasternack, L. R.; McDonald, J. R. *Chem. Phys.* **1980**, *48*, 203-208.

(13) Müller, R. P.; Russegger, P.; Huber, J. R. *Chem. Phys.* **1982**, *70*, 281-290.

(14) Müller, R. P.; Huber, J. R. *J. Mol. Spectrosc.* **1984**, *104*, 209-225.

(15) King, D. S.; Stephenson, J. C. *J. Chem. Phys.* **1985**, *82*, 2236-2239.

(16) Cox, A. P.; Waring, S. J. *Chem. Soc., Faraday Trans.* **1972**, *2*, 1060-1070.

(17) Rook, F. L.; Jacox, M. E. *J. Mol. Spectrosc.* **1982**, *93*, 101-106.

(18) Ghosh, P. N.; Bauder, A.; Gunthard, H. H. *Chem. Phys.* **1980**, *53*, 39-50.

(19) Turner, P. H.; Corkill, M. J.; Cox, A. P. *J. Phys. Chem.* **1979**, *83*, 1473-1482.

(20) Bondybey, V. E.; English, J. H. *J. Mol. Spectrosc.* **1982**, *92*, 431-442.

(21) Flicker, W. M.; Mosher, O. A.; Kuppermann, A. *J. Chem. Phys.* **1980**, *72*, 2788-2794.

(22) (a) Lazaar, K. I.; Bauer, S. H. *J. Phys. Chem.* **1984**, *88*, 3052-3059.

(b) Chauvel, J. P.; Friedman, B. R.; Van, H.; Winegar, E. D.; True, N. S. *J. Chem. Phys.* **1985**, *82*, 3996-3998. Chauvel, J. P.; Friedman, B. R.; True, N. S.; Winegar, E. D. *Chem. Phys. Lett.* **1985**, *122*, 175-179.

(23) Yamada, F.; Slagle, I. R.; Gutman, D. *Chem. Phys. Lett.* **1981**, *53*, 409-412.

(24) Cassady, C. J.; Freiser, B. S.; McElvany, S. W.; Allison, J. *J. Am. Chem. Soc.* **1984**, *106*, 6125-6134.

(25) Kleier, D. A.; Lipton, M. A. *THEOCHEM.* **1984**, *109*, 39-49.

(26) Marynick, D. S.; Ray, A. K.; Fry, J. L.; Kleier, D. A. *THEOCHEM* **1984**, *108*, 45-48. Marynick, D. S.; Ray, A. K.; Fry, J. L. *Chem. Phys. Lett.* **1985**, *116*, 429-433.

Table I. Total Energies (-hartrees) and Zero Point Energies (kcal/mol) of Various Species on the CH<sub>3</sub>NO<sub>2</sub> Potential Energy Surface<sup>a</sup>

molecule	mol/elec symmetry	3-21G// 3-21G	6-31G// 6-31G*	6-31G*// 6-31G*	MP2/6-31G <sup>a</sup> // 6-31G*	MP2/6-31G <sup>bb</sup> // 6-31G*	ZPE/3-21G <sup>c</sup>	ZPE/6-31G <sup>c</sup>	
1	CH <sub>3</sub> NO <sub>2</sub>	C <sub>s</sub>	242.255 86	243.523 38	243.661 99	243.996 77	244.337 94	32.58 (0)	34.25 (0)
2	CH <sub>3</sub> NO <sub>2</sub>	C <sub>s</sub>	242.255 85	243.523 36	243.661 98	243.996 76	244.337 92	32.55 (1)	34.21 (1)
3	CH <sub>3</sub> ONO	C <sub>s</sub>	242.280 34	243.527 87	243.665 71	243.983 81	244.327 24		33.13 (1)
4	CH <sub>3</sub> ONO	C <sub>s</sub>	242.280 77	243.527 93	243.666 31	243.982 74	244.326 60		32.23 (0)
5	CH <sub>3</sub> ONO	C <sub>s</sub>	242.282 65	243.525 93	243.664 20	243.983 18	244.327 74		33.29 (1)
6	CH <sub>3</sub> ONO	C <sub>s</sub>	242.286 36	243.528 76	243.668 64	243.985 57	244.331 48		33.69 (0)
7	CH <sub>3</sub> ONO	C <sub>1</sub>	242.270 64	243.513 25	243.650 28	243.965 42	244.307 81	31.79 (1)	32.78 (1)
8	CH <sub>2</sub> N(O)OH	C <sub>s</sub>	242.255 41	243.506 88	243.629 62	243.964 90	244.302 77		32.99 (0)
9	CH <sub>2</sub> N(O)OH	C <sub>s</sub>	242.231 61	243.486 96	243.613 50	243.950 30	244.289 88		33.58 (0)
10	CH <sub>2</sub> N(O)OH	C <sub>s</sub>	242.133 50	243.377 10	243.522 82	243.838 10	244.189 18		31.71 (1)
11	CH <sub>2</sub> (OH)NO	C <sub>s</sub>	242.299 68	243.552 89	243.681 85	243.994 80	244.333 98	32.29 (0)	33.40 (1)
12	CH <sub>2</sub> (OH)NO	C <sub>s</sub>	242.293 40	243.549 83	243.676 21	255.991 06	244.326 44	31.70 (1)	32.99 (1)
13	CH <sub>2</sub> (OH)NO	C <sub>s</sub>		243.553 28	243.681 93	243.995 07	244.335 74		33.58 (0)
14	CH <sub>2</sub> (OH)NO	C <sub>s</sub>	242.288 99	243.546 17	243.673 87	243.987 15	244.324 28		33.29 (0)
15	CH <sub>2</sub> (OH)NO	C <sub>s</sub>	242.288 70	243.545 70	243.673 87	243.986 74	244.323 46		33.03 (1)
16	CH <sub>2</sub> (OH)NO	C <sub>1</sub>		243.546 30	243.673 79	243.987 28	244.324 21		33.14 (1)
17	CH <sub>2</sub> (OH)NO	C <sub>1</sub>		243.540 29	243.667 78	243.981 71	244.318 36		33.12 (2)
18	CH <sub>2</sub> ONO	C <sub>1</sub>	242.253 04	243.481 46	243.623 72	243.928 10	244.288 06		34.13 (0)
19	TS <sub>1</sub>	C <sub>1</sub>	242.127 55 <sup>d</sup>	243.367 56	243.486 83	243.823 86	244.159 71	30.00 (1)	30.74 (1)
20	TS <sub>2</sub>	C <sub>1</sub>	242.142 62	243.385 20	243.508 18	243.860 64	244.199 51	30.34 (1)	31.80 (1)
21	TS <sub>3</sub>	C <sub>1</sub>	242.143 69 <sup>e</sup>	243.401 22	243.531 94	243.881 58	244.216 24	30.32 (1)	31.39 (1)
22	SS <sub>4</sub> <sup>f</sup>	C <sub>s</sub>	242.138 94	243.385 50	243.527 35	243.861 80	244.211 17	27.95 (1)	29.66 (2)
23	TS <sub>4</sub> <sup>f</sup>	C <sub>1</sub>	242.162 78 <sup>g</sup>	243.408 10	243.549 19	243.918 16	244.253 19	28.10 (1)	28.62 (1)
24	NO <sub>2</sub> + CH <sub>3</sub>	<sup>2</sup> A <sub>1</sub> , <sup>2</sup> A <sub>2</sub> <sup>h</sup>			243.590 48		244.232 61		25.61 (0)
25	HNO + H <sub>2</sub> C=O	<sup>1</sup> A <sub>1</sub> , <sup>1</sup> A <sub>1</sub>			243.652 40		244.296 91		28.40 (0)
26	CH <sub>2</sub> NO <sub>2</sub> + H	<sup>2</sup> B <sub>1</sub> , <sup>2</sup> S			243.528 05		244.175 82		24.41 (0)
27	NO + OCH <sub>3</sub>	<sup>2</sup> Π, <sup>2</sup> A <sup>h</sup>			243.668 50		244.255 48		27.48 (1)
28	H <sub>2</sub> O + HNCO	<sup>1</sup> A <sub>1</sub> , <sup>1</sup> A <sub>1</sub>			243.772 13		244.426 84		28.72 (0)
29	H <sub>2</sub> O + HCNO	<sup>1</sup> A <sub>1</sub> , <sup>1</sup> Σ <sup>+</sup>			243.641 18		244.318 56		28.85 (0)
30	ONOH + CH <sub>2</sub>	<sup>1</sup> A <sub>1</sub> , <sup>1</sup> A <sub>1</sub>			243.512 31		244.141 84		25.80 (0)

<sup>a</sup>Frozen core approximation. <sup>b</sup>All orbitals included in correlation treatment. <sup>c</sup>Number of negative vibrational frequencies is given in parentheses.

<sup>d</sup>A stationary point of C<sub>s</sub> symmetry 46.3 kcal/mol less stable was located and found to have two imaginary frequencies. <sup>e</sup>A stationary point of C<sub>s</sub> symmetry 3.0 kcal/mol less stable was located and found to have two imaginary frequencies. <sup>f</sup>Super Saddle point. <sup>g</sup>A stationary point of C<sub>s</sub> symmetry 11.5 kcal/mol less stable was located and found to have two imaginary frequencies. <sup>h</sup>Electronic state symmetries of fragments.

<sup>i</sup>Calculations at all levels are at 6-31G\* optimized geometries except those reported at the 3-21G level, which are optimized at 1 that level.

of the aci forms,<sup>28</sup> conformational stabilities in methyl nitrite,<sup>29</sup> charge distributions,<sup>30</sup> and vibrational frequencies.<sup>31</sup> Also, a MNDO study of rearrangements in 1-nitropropene has been reported.<sup>32</sup>

The most thorough study of thermolysis of molecules containing NO<sub>2</sub> groups is a recent MINDO/3 study by Dewar and co-workers.<sup>33</sup> Their use of MINDO/3 rather than MNDO is surprising since the latter method is normally better suited for systems containing adjacent lone pairs. If the experimental heat of formation is used for NO<sub>2</sub>, the C-N bond energy of CH<sub>3</sub>NO<sub>2</sub> is well reproduced<sup>33</sup> (calcd 59.5; obsd 60.0 kcal/mol) as well as the O-N bond energy in CH<sub>3</sub>ONO (calcd 40.4; obsd 42.1 kcal/mol). However, their reported barriers for the nitromethane to methyl nitrite rearrangement (47.0 kcal/mol) and methyl nitrite decomposition to formaldehyde plus nitroxyl (32.4 kcal/mol) are much lower than those found in the present study. Since the rearrangement barriers they calculated are smaller than the C-N bond energy in the CH<sub>3</sub>NO<sub>2</sub> → CH<sub>3</sub>ONO reaction and smaller than the O-N bond energy in the CH<sub>3</sub>ONO → O=CH<sub>2</sub> + HNO reaction, they conclude that the concerted rearrangement will be favored over (or competitive with) simple bond fission. In the present study, rearrangements are predicted to have barriers higher

than bond energies which leads to the conclusion that the reactions must be either bimolecular or proceed by initial bond cleavage.

In addition to determining rearrangement barriers, the present study will be undertaken to analyze several rotamers of stable species on the CH<sub>3</sub>NO<sub>2</sub> potential energy surface. Since a major goal of theoretical chemistry is to provide data to the experimentalist that is otherwise difficult to obtain, a comparison of the relative energies of the rotamers will aid in interpreting microwave data. An analysis of the vibrational frequencies of several CH<sub>3</sub>NO<sub>2</sub> species will follow in a separate article.

## Methods

All calculations have been made by using the GAUSSIAN 82 program system.<sup>34</sup> Geometries have been optimized by using the 3-21G and the 6-31G\* basis sets. By using the 6-31G\* geometries, the polarization increment (6-31G\*) and correlation increment (MP2/6-31G) starting from the 6-31G basis set have been made in order to determine relative energies at the additivity level ([MP2/6-31G\*]). The additivity approximation (eq 13) has been tested and shown to yield relative energies

$$\Delta E[\text{MP2/6-31G}^*] = \Delta E(\text{MP2/6-31G}) + \Delta E(\text{HF/6-31G}^*) - \Delta E(\text{HF/6-31G}) \quad (13)$$

normally within 5 kcal/mol of those from the full basis set.<sup>35</sup> Despite

(27) Chabalowski, C.; Hariharan, P. C.; Kaufman, J. J. *Int. J. Quantum Chem.* **1983**, *17*, 643-644.

(28) Murrell, J. N.; Vidal, B.; Guest, M. F. *J. Chem. Soc., Faraday Trans.* **1975**, *2*, 1577-1582.

(29) Cordell, F. R.; Boggs, J. E.; Skancke, A. *J. Mol. Struct.* **1980**, *64*, 57-65.

(30) Ritchie, J. P. *J. Am. Chem. Soc.* **1985**, *107*, 1825-1837.

(31) McKee, M. L. *J. Am. Chem. Soc.* **1985**, *107*, 1900-1904. The calculated MNDO isotope frequency shifts were incorrectly reported in this paper for the b<sub>1</sub> and b<sub>2</sub> modes of CD<sub>2</sub>NO<sub>2</sub>. The correct shifts for the b<sub>1</sub> modes are -133 and -34 cm<sup>-1</sup>, while for the b<sub>2</sub> modes the correct shifts are -878, -2, -235, and -45 cm<sup>-1</sup>.

(32) Turner, A. G.; Davis, L. P. *J. Am. Chem. Soc.* **1984**, *106*, 5447-5451.

(33) Dewar, M. J. S.; Ritchie, J. P.; Alster, J. J. *Org. Chem.* **1985**, *50*, 1031-1036.

(34) References to basis sets used are collected here. The program package GAUSSIAN 82 was used throughout. Carnegie-Mellon University: Binkley, J. S.; Frisch, M.; Raghavachari, K.; Fluder, E.; Seeger, R.; Pople, J. A. 3-21G basis: Binkley, J. S.; Pople, J. A.; Hehre, W. J. *J. Am. Chem. Soc.* **1980**, *102*, 939. 6-31G basis: Hehre, W. J.; Ditchfield, R.; Pople, J. A. *J. Chem. Phys.* **1972**, *56*, 2257. 6-31G\* basis: Hariharan, P. C.; Pople, J. A. *Theor. Chim. Acta* **1973**, *28*, 213. Gordon, M. S. *Chem. Phys. Lett.* **1980**, *76*, 163. Francl, M. M.; Pietro, W. J.; Hehre, W. J.; Binkley, J. S.; Gordon, M. S.; Defrees, D. J.; Pople, J. A. *J. Chem. Phys.* **1977**, *77*, 3654. MP2 correlation treatment: Moller, C.; Plesset, M. S. *Phys. Rev.* **1934**, *45*, 618. Pople, J. A.; Binkley, J. S.; Seeger, R. *Int. J. Quantum Chem., Symp.* **1979**, *13*, 225.

(35) McKee, M. L.; Lipscomb, W. N. *J. Am. Chem. Soc.* **1981**, *103*, 4673-4676. Nobes, R. H.; Bouma, W. J.; Radom, L. *Chem. Phys. Lett.* **1982**, *89*, 497-500. McKee, M. L.; Lipscomb, W. N. *Inorg. Chem.* **1985**, *24*, 762-764.

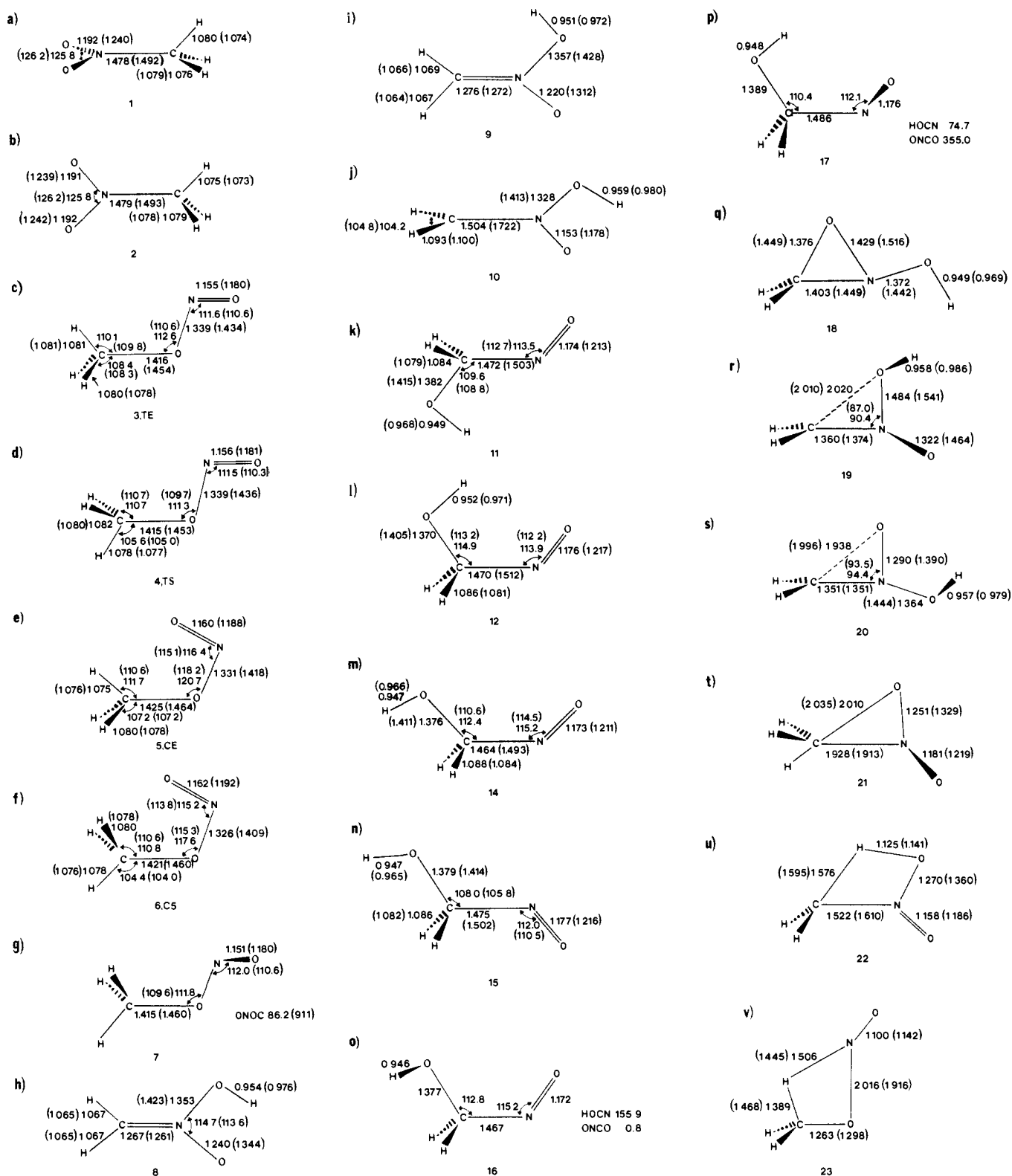


**Figure 1.** Geometric parameters of relevant species on the  $\text{CH}_3\text{NO}_2$  potential energy surface at the 3-21G and 6-31G\* levels. Values at the 3-21G level are in parentheses.

its general success, in the present application the additivity approximation is found not to be accurate due to the multiconfigurational nature of the  $\text{CH}_3\text{NO}_2$  surface.<sup>36</sup>

Vibrational frequencies are calculated analytically by using the CPHF method at the 6-31G\* and 3-21G levels to characterize stationary points

and calculate zero point corrections. Total energies (hartrees) of all species are presented in Table I, relative energies (kcal/mol) are presented in Table II, and relevant geometric data are presented in Figure 1. Species notation used in Tables I and II and Figure 1 are maintained consistently throughout.

The discussion of results will be divided into three sections. First, the stable isomers and related conformers will be discussed. Next, results for concerted rearrangements will be presented, and the origins of high barriers will be analyzed. Lastly, possibly fragmentation pathways will be explored from the perspective of reaction enthalpies.

(36) A limitation of the method is also found for open shell systems in which the correct spin-squared value is not obtained. McKee, M. L. *J. Phys. Chem.* **1986**, *90*, 2335-2340.

Table II. Relative Energy (kcal/mol) of Various Species on the  $\text{CH}_3\text{NO}_2$  Potential Energy Surface

molecule	6-31G// 6-31G*	6-31G*// 6-31G*	MP2/6-31G// 6-31G*	[MP2/6-31G*] <sup>a</sup> // 6-31G*	MP2/6-31G*// 6-31G*	MP2/6-31G* + ZPC// 6-31G*	exptl <sup>b</sup>
1 $\text{CH}_3\text{NO}_2$	0	0	0	0	0	0	0
2 $\text{CH}_3\text{NO}_2$	0.01	0.01	0.01	0.01	0.01	-0.03	
3 $\text{CH}_3\text{ONO}$	-2.82	-2.33	8.13	8.62	6.71	5.59	
4 $\text{CH}_3\text{ONO}$	-2.85	-2.71	8.80	8.94	7.12	6.10	
5 $\text{CH}_3\text{ONO}$	-1.60	-1.39	8.53	8.74	6.40	5.44	
6 $\text{CH}_3\text{ONO}$	-3.38	-4.17	7.03	6.24	4.05	3.49	2.3
7 $\text{CH}_3\text{ONO}$	6.36	7.35	19.67	20.66	18.91	17.44	15.19 <sup>c</sup>
8 $\text{CH}_2\text{N}(\text{O})\text{OH}$	10.35	20.31	20.00	29.96	22.07	21.81	
9 $\text{CH}_2\text{N}(\text{O})\text{OH}$	22.85	30.43	29.16	36.74	30.16	29.49	
10 $\text{CH}_2\text{N}(\text{O})\text{OH}$	91.79	87.33 <sup>d</sup>	99.56	95.10	93.34 <sup>d</sup>	90.80	
11 $\text{CH}_2(\text{OH})\text{NO}$	-18.52	-12.46	1.24	7.30	2.48	1.63	
12 $\text{CH}_2(\text{OH})\text{NO}$	-16.60	-8.92	3.58	11.26	7.22	5.96	
13 $\text{CH}_2(\text{OH})\text{NO}$	-18.76	-12.51	1.07	7.32	2.64	1.97	
14 $\text{CH}_2(\text{OH})\text{NO}$	-14.30	-7.45	6.04	12.89	8.57	7.61	
15 $\text{CH}_2(\text{OH})\text{NO}$	-14.00	-7.45	6.29	12.84	9.09	8.87	
16 $\text{CH}_2(\text{OH})\text{NO}$	-14.38	-7.40	5.95	12.93	8.62	7.51	
17 $\text{CH}_2(\text{OH})\text{NO}$	-10.61	-3.63	9.45	16.43	12.29	11.16	
18 $\text{CH}_2\text{ONOH}$	26.30	24.01	43.09	40.80	31.30	31.18	
19 $\text{TS}_1$	97.78	109.91	108.50	120.63	111.84	108.33	
20 $\text{TS}_2$	86.71	96.51	85.42	95.22	86.86	84.41	
21 $\text{TS}_3$	76.65	81.60	72.28	77.23	76.36	73.50	
22 $\text{SS}_4$	86.52	84.48	84.69	82.65	79.55	74.96	
23 $\text{TS}_5$	72.34	70.78	49.33	47.77	53.18	47.55 <sup>e</sup>	
24 $\text{NO}_2 + \text{CH}_3$		44.87			66.09	57.45	60.1 (58.5) <sup>f</sup>
25 $\text{HNO} + \text{H}_2\text{C}=\text{O}$		6.02			25.74	19.89	15.7
26 $\text{CH}_2\text{NO}_2 + \text{H}$		84.04			101.73	91.89	107.5 <sup>g</sup>
27 $\text{NO} + \text{OCH}_3$		-4.08			51.84	44.97	43.0 (43.5) <sup>f</sup>
28 $\text{H}_2\text{O} + \text{HNCO}$		-69.11			-55.78	-61.31	[-69.9]
29 $\text{H}_2\text{O} + \text{HCNO}$		13.06			12.16	4.94	
30 $\text{ONOH} + \text{CH}_2$		93.92			123.05	114.60	95.6 <sup>h</sup>

<sup>a</sup> Additivity approximation. (See text.) <sup>b</sup> Unless otherwise noted enthalpies are from Benson, S. W. *Thermochemical Kinetics*, 2nd ed.; John Wiley: New York, 1976. For purposes of comparing, the experimental energies are compared relative to nitromethane, 1. <sup>c</sup> The experimental torsion barrier (11.70 kcal/mol, ref 22b) is added to the calculated relative energy of the lowest conformation of  $\text{CH}_3\text{ONO}$  (3.49 kcal/mol). <sup>d</sup> A UHF/6-31G\* solution 10.96 kcal/mol lower in energy was obtained starting with singly occupied orbitals on carbon and nitrogen. However at the UMP2/6-31G\* level, this solution yields an energy 24.92 kcal/mol higher than the MP2/6-31G\* energy. <sup>e</sup> The  $\text{C}_2$  stationary point (two imaginary frequencies) for elimination was 8.5 kcal/mol higher at the MP2/6-31G\* + ZPC//6-31G\* level. <sup>f</sup> Reference 1. <sup>g</sup> Reference 46 for heat of formation of  $\text{CH}_2\text{NO}_2$ . <sup>h</sup> Heat of formation of  $\text{CH}_2(^1\text{A}_1)$  is taken as 96 kcal/mol.

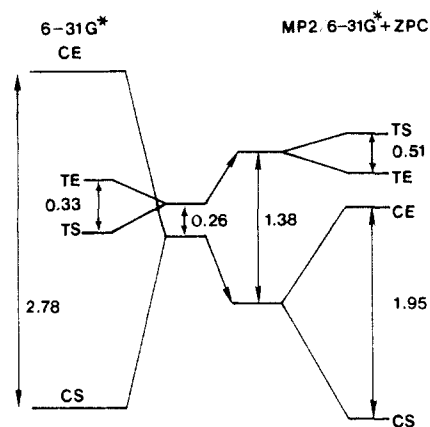


Figure 2. Diagram of conformational stabilities (kcal/mol) of methyl nitrite at the 6-31G\* level (left) and at the MP2/6-31G\* + ZPC level (right). The average of the eclipsed and staggered methyl conformations are given at the respective levels.

### Conformational Surface

**Nitromethane,  $\text{CH}_3\text{NO}_2$ .** The two orientations of the methyl group (staggered and eclipsed) are predicted to be very close in energy which is in agreement with an unusually small observed torsional barrier.<sup>16</sup> A detailed analysis of theoretical results for  $\text{CH}_3\text{NO}_2$  has been made<sup>31</sup> and will not be repeated.

It is interesting to observe (Table II) the close balance between an attractive dominant barrier which would favor the eclipsed conformer 2 and a repulsive dominant<sup>37</sup> barrier which would favor the staggered conformer 1. The staggered conformer is predicted

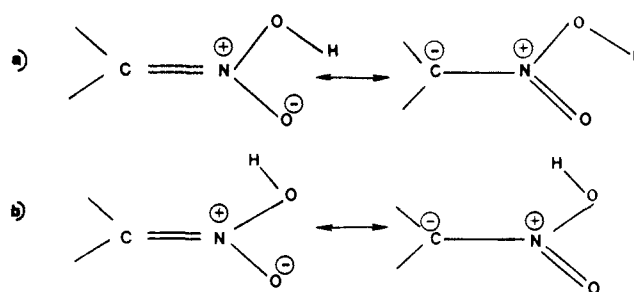
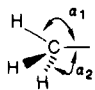


Figure 3. Two resonance forms of *cis*- and *trans*-*aci*-nitromethane. The *cis* form (internal hydrogen bond to oxygen) increases the contribution of the resonance structure with the  $\text{C}=\text{N}$  double bond relative to the *trans* form.

to be slightly more stable at all levels. However, inclusion of zero point energy provides a slight advantage to the eclipsed conformer. The calculated difference (0.03 kcal/mol) is not considered to be reliable at this level of theory.

**Methyl Nitrite,  $\text{CH}_3\text{ONO}$ .** The methyl rotational barriers of *cis* and *trans* methyl nitrite are known to be substantially different. The barrier in the *cis* conformer is 2.10 kcal/mol;<sup>18</sup> while in the *trans* conformer, it is less than 0.30 kcal/mol (0.27 kcal/mol;<sup>18</sup> 0.03 kcal/mol<sup>19</sup>). On the basis of calculations at the 4-21G level good agreement with the observed barriers is obtained;<sup>29</sup> however, higher level calculations performed here lead to a modified interpretation. In Figure 3 data are presented on the left for results at the 6-31G\* level and on the right for results at the MP2/6-31G\* + ZPC level. For clarity, the average of the staggered and eclipsed methyl conformation for *cis* and for *trans* methyl nitrite (abbreviated CS, CE, TS, and TE) are presented. At the 6-31G\* level the average *cis* conformer (CS and CE) is 0.3 kcal/mol more stable than the average of the *trans* conformer (TS and TE), and

(37) Allen, L. C. *Chem. Phys. Lett.* **1968**, *2*, 597-601.

**Table III.** Methyl Group Tilt (deg) in CH<sub>3</sub>ONO Conformers at the 3-21G and 6-31G\* Levels<sup>a</sup>


confrmtn	3-21G			6-31G*		
	$\alpha_1$	$\alpha_2$	$\frac{\alpha_1 - (\alpha_1 + 2\alpha_2)/3}{}$	$\alpha_1$	$\alpha_2$	$\frac{\alpha_1 - (\alpha_1 + 2\alpha_2)/3}{}$
TE, <sup>b</sup> <b>3</b>	109.8	108.3	1.0	110.1	108.4	1.1
TS, <b>4</b>	105.0	110.7	-3.8	105.6	110.7	-3.4
CE, <b>5</b>	110.6	102.7	2.3	111.7	107.2	3.0
CS, <b>6</b>	104.0	110.6	-4.4	104.4	110.8	-4.3

<sup>a</sup>The direction of the methyl tilt is in every case away from the nitrogen. <sup>b</sup>Denotes conformation of CH<sub>3</sub>ONO, *trans*- or *cis*-methyl nitrite and eclipsed or staggered methyl group.

this value is increased to 1.4 kcal/mol at the MP2/6-31G\* + ZPC level. The splitting due to methyl rotation in the *cis* conformer decreases from 2.8 kcal/mol at the 6-31G\* level to 2.0 kcal/mol at the MP2/6-31G\* + ZPC level. The latter value agrees well with the experimental difference of 2.10 kcal/mol. The staggered conformation (CS) is the most stable orientation at both levels. It has been pointed out<sup>29</sup> that this conformation allows a particularly favorable hyperconjugative interaction of the out-of-plane CH<sub>2</sub> group with the N=O double bond. The present calculations indicate however that this is not the dominant mode of stabilization in the CS conformation.

In the *trans* conformer, the methyl group is predicted to be more stable in a staggered (TS) orientation than an eclipsed (TE) by 0.3 kcal/mol. At the higher level of calculation (MP2/6-31G\* + ZPC) the stabilities are reversed resulting in the eclipsed orientation 0.5 kcal/mol more stable than the staggered.

In the *cis* and *trans* conformers, the eclipsed conformers (CE and TE) are predicted to be stabilized relative to the staggered (CS and TS) by 0.8 kcal/mol and 0.9 kcal/mol, respectively, when correlation is introduced. The probable cause is due to an overestimation of hyperconjugation of the out-of-plane CH<sub>2</sub> group with the N=O double bond which involves the occupied CH<sub>3</sub>  $\pi$ -type orbital interacting with the empty  $\pi^*$  C=N orbital. A MCSCF treatment would yield an appreciable occupation of the  $\pi^*$  C=N orbital which would reduce the amount of hyperconjugative stabilization. Similarly, the inclusion of correlation will also have the effect of reducing hyperconjugation. Clearly the energy difference in the TE and TS methyl orientation will be very sensitive to the level of calculations. It is interesting, however, that the most stable orientation of the methyl group is staggered in the *cis* conformer and eclipsed in the *trans* conformer.

Another source of comparison among the various conformers is the direction and degree of methyl group tilt.<sup>38,39</sup> If hyperconjugation is important, the methyl group should tilt toward the terminal oxygen or equivalently in the direction of increasing overlap of the interacting orbitals. If the dominant interacting orbitals are the empty  $\pi^*$  orbital of CH<sub>3</sub> and the occupied  $\pi$  orbital of ONO (mostly on the oxygen adjacent to the methyl group), the methyl group tilt should be in the direction that increases the HCO angle of the unique hydrogen in the CS conformer (Figure 1f). The tilt angles given in Table IV indicate instead a tilt away from nitrogen in order to reduce steric repulsion. Hyperconjugative effects may explain why the methyl tilt is not greater in TE and CE compared to TS and CS since in the eclipsed orientation steric repulsion might be thought to be larger.

Cordell et al. suggest<sup>29</sup> that the TE conformer (Figure 1c) is strongly stabilized by an attractive interaction between CH<sub>1</sub> (unique hydrogen) and the lone pair on the nitrogen atom. Evidence is taken from the small HC<sub>1</sub>N angle (4-21G, 104.7°). Such

**Table IV.** Comparison of Mulliken Charges and Structural Parameters for *cis*-**8** and *trans*-**9** *aci*-Nitromethane at the 6-31G\* Level

	<i>cis</i> - <b>8</b>	<i>trans</i> - <b>9</b>	<i>trans</i> - <i>cis</i>
Mulliken Charges (e <sup>-</sup> )			
C	-0.24	-0.30	-0.06
N	0.46	0.48	0.02
O <sup>a</sup>	-0.61	-0.55	0.06
Bond Distances (Å)			
C-N	1.267	1.276	0.009
N-O <sup>a</sup>	1.240	1.220	-0.020

<sup>a</sup>Singly coordinated oxygen.

an interpretation is not warranted from the present calculations as evidenced from the much larger calculated H<sub>1</sub>CO angle (6-31G\*, 110.1°). In fact the close correspondence between the result of Cordell et al. and the present work at the 3-21G level if the TS and TE geometries of Cordell et al. are interchanged leads the present author to suggest that their geometries have been incorrectly assigned.

The average *cis* conformer is predicted to be more stable than the average *trans* conformer by 1.4 kcal/mol. For comparison, high level calculations of HONO predict<sup>40</sup> that the *cis* conformer is favored by 0.8 kcal/mol. Of the two methyl group orientations in the *cis* conformer the staggered orientation is most easily rationalized by the reduction of steric crowding. The methyl orientation in the *trans* conformer is sensitive to the level of calculation. Here, steric effects may be less important, or a counterbalance of bond pair repulsion may exist. In this case hyperconjugation may be responsible for the preferred orientation.

A transition structure of C<sub>1</sub> symmetry (**7**, Figure 1g) connecting the CS and TS conformers was located on the 3-21G and 6-31G\* potential energy surfaces. The barrier was calculated to be 14.0 kcal/mol at the MP2/6-31G\* + ZPC level which compares well with the observed<sup>22b</sup> barrier of 11.7 kcal/mol.

**CH<sub>2</sub>N(O)OH *aci*-Nitromethane.** Two conformers of *aci*-nitromethane were investigated, the *cis* (**8**) and *trans* (**9**) conformers, where *cis* and *trans* indicate the relation of the hydroxyl group relative to NO. Two resonance structures can be written for each (Figure 3) which involve exchanging the position of the double bond. The *cis* conformer is favored by 7.7 kcal/mol relative to the *trans* due to stabilization from the internal hydrogen bond. It is also seen that the *cis* conformer is dominated more by the resonance structure containing a C=N bond (Figure 3a) compared to the *trans* conformer. The Mulliken charges of C, N, and O as well as the C=N and NO bond distances are compared for both conformers in Table IV. The *cis* conformer is characterized by a more negative oxygen, a more positive carbon, a shorter C=N bond, and a longer NO bond compared to the *trans* conformer, which point to a greater contribution from the resonance structure on the left in Figure 3a in the *cis* conformer.

Murrell, Vidal, and Guest have reported<sup>28</sup> calculations which indicate that at the double- $\zeta$  level and using assumed geometries *aci*-nitromethane is more stable than nitromethane in contradiction to observations. The present calculations correctly predict *aci*-nitromethane to be less stable, and at the MP2/6-31G\* + ZPC level the difference is 21.8 kcal/mol. *Ac*i-nitromethane has been proposed as the first product in the protonation of the nitromethyl anion which slowly rearranges to nitromethane, a pseudo acid. The hydrogen migration in *aci*-nitromethane is predicted to have a high barrier (vide infra) indicating that the concerted mechanism is unlikely.

**Nitrosomethanol, CH<sub>2</sub>(NO)OH.** Until very recently the species CH<sub>2</sub>(NO)OH was unknown.<sup>10,11,14</sup> Several spectroscopic studies have appeared for *cis*- and *trans*-nitrosomethanol, but the conformational potential energy surface is unexplored. The present theoretical study may provide valuable information if a microwave structure determination is attempted.

Four conformers of nitrosomethanol with C<sub>s</sub> symmetry have been determined (**11**, **12**, **14**, and **15**) as well as several with only

(38) Radom, L. *Structural Consequences of Hyperconjugation In Molecular Structure and Conformation*; Czismadia, I. G., Ed.; Elsevier: New York, 1982; pp 1-64.

(39) Radom, L.; Baker, J.; Gill, P. M. W.; Nobes, R. H.; Riggs, N. V. *THEOCHEM* **1985**, 126, 271-290.

(40) Turner, A. G. *J. Phys. Chem.* **1985**, 89, 4480-4483.

**Table V.** Comparison of Conformation Energies (kcal/mol) for the Nitrosomethanol Potential Energy Surface at the MP2/6-31G\* + ZPC and STO-3G Levels

confrmtn	MP2/6-31G* + ZPC	STO-3G <sup>a</sup>
CC, <sup>b</sup> <b>11</b>	0.0	0.0
CT, <b>12</b>	4.3	2.9
TC, <b>14</b>	6.0	2.9
TT, <b>15</b>	7.2	4.5

<sup>a</sup>Reference 14. <sup>b</sup>Notation refers to OH orientation relative to the C-N bond (cis or trans) and to the O-C orientation relative to the N=O bond (cis or trans).

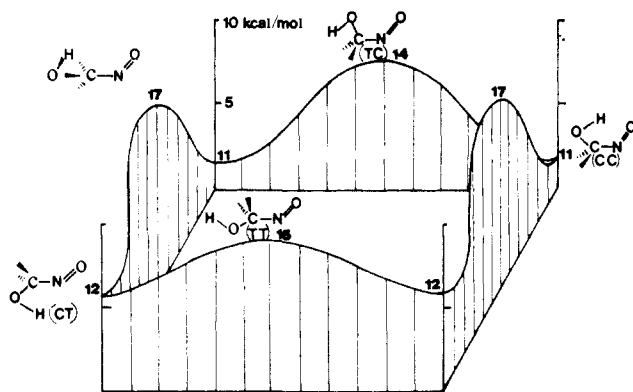


**Figure 4.** Potential energy surface of nitrosomethanol at the 6-31G\* + ZPC level. CC and CT are stable conformations while TC and TT represent transition structures. In the perspective cube, the front and back Minimum Energy Reaction Profiles correspond to rotation about the C-O bond while the side profiles correspond to rotation about the C-N bond. A  $C_1$  symmetry transition structure 11.2 kcal/mol less stable than  $\text{CH}_3\text{NO}_2$  allows rearrangement of the CC and CT conformation.

$C_1$  symmetry. The relative energies of the nitrosomethanol conformers are summarized in Table V along with calculations at the STO-3G level<sup>14</sup> which are quite successful in reproducing the results at the higher level. The potential energy surface is illustrated in Figure 4 which indicates two stable conformers **11** and **12** corresponding to *syn, cis*- and *syn, trans*-nitrosomethanol. At the 6-31G\* level, the *syn-cis* structure **11** is predicted to be a transition structure to another structure **13** in which the OCNO and HOCN dihedral angles are 9.5 and 26.5°, respectively. The  $C_1$  structure **13** is only 0.05 kcal/mol more stable than **11** at the 6-31G\* level, and the stability is reversed at the MP2/6-31G\* + ZPC level indicating that the unsymmetrical minimum **13** disappears at high levels of computation leaving **11** as the true minimum. A similar discrepancy occurs for **14** which is predicted at the 6-31G\* level to be in a local minimum. The transition structure **16** connecting **14** and **12** is only 0.05 kcal/mol higher than **14** and is characterized by OCNO and HOCN dihedral angles of 0.8 and 24.0°, respectively. At the MP2/6-31G\* + ZPC level the  $C_s$  structure **14** is predicted to be less stable than the transition structure suggesting that **14** should be a transition structure rather than a minimum at the MP2/6-31G\* + ZPC level. These two situations are depicted in Figure 5.

In this regard, it is interesting to note a similar phenomenon<sup>39,41</sup> found for the rotational barrier of  $\text{NH}_2\text{-NH}_2$ . The anti form is found to lie in a very shallow local minimum (less than 0.1 kcal/mol barrier). In contrast to the present system, the barrier was found to persist up to MP2/6-31G\*//6-31G\* albeit still in a very shallow well.

Rotational barriers were determined around the C-O bond in both the *syn, cis* **11** and *syn, trans* **12** conformers of nitrosomethanol (Figure 4). The rotational barrier in **11** (**11** → **14** → **11**) is expected and found to have a higher barrier than in **12** (**12** → **15** → **12**) (6.0 kcal/mol and 2.9 kcal/mol, respectively), since in the former case an internal hydrogen bond is formed. However,

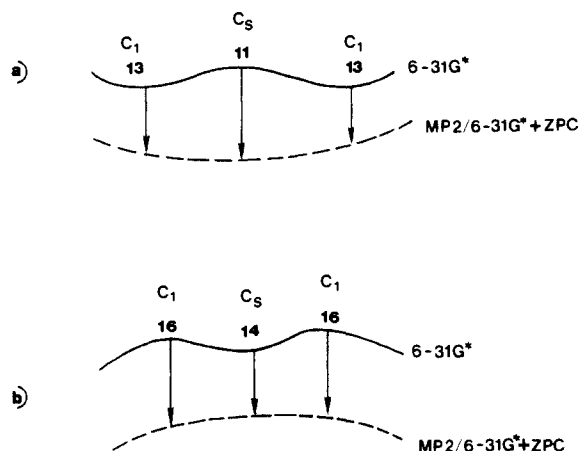


**Figure 5.** The upper surface represents stationary points characterized by calculating force constants at the 6-31G\* level. The dashed curve gives the order of stabilities at the MP2/6-31G\* + ZPC level and suggests that a qualitative change has taken place. In Figure 5a, the  $C_s$  transition structure **11** is predicted to be more stable than **13** at the higher level while in Figure 5b, the  $C_s$  minimum structure **14** is predicted to be less stable than **16** at the higher level.

even in the *trans* conformer there will be some hydrogen bonding to the nitrogen, and hence the 3.1 kcal/mol difference in the rotational barrier will represent the lower limit to the strength of the internal hydrogen bond. For a related molecule, nitrosomethane, it has been determined experimentally<sup>42</sup> that the lowest energy conformation is an eclipsed methyl group with a rotational barrier of 1.1 kcal/mol.

It is possible to selectively photoisomerize *cis* → *trans* or *trans* → *cis* depending on the wavelength used.<sup>10,11,14</sup> This indicates that thermal isomerization of **11** → **12** must be slow at the temperature of the experiment (20 K) since otherwise an identical equilibrium would be reestablished. A barrier of 9.6 kcal/mol is calculated for rotation around the C-N bond (**11** → **17** → **12**), and a 5.2 kcal/mol barrier is calculated in the reverse direction (**12** → **17** → **11**). At 20 K, a 5.2 kcal/mol barrier is sufficient to prevent rapid isomerization. It is to be noted that the force constant matrix of **17**, the stationary point interconverting **11** and **12**, has two negative eigenvalues (Table I). The transition vector of one negative eigenvalue corresponds to the expected rotation of the nitroso group about the CN bond, while the second transition vector corresponds to a rotation of the hydroxyl group out of the approximate HOCN plane. Since on two occasions, rotation of the hydroxyl group about the CO bond has led to spurious stationary points, a structure with one negative eigenvalue was not located.

### Rearrangements on the $\text{CH}_3\text{NO}_2$ Surface

One of the questions being addressed here is whether any concerted rearrangement barriers are competitive with radical formation and recombination. Both photolysis and pyrolysis of nitromethane are generally regarded to occur by an initial fission of the C-N bond. However, in the photolysis of nitromethane, the excited singlet might have time to rearrange to a geometry on the product side of the thermal barrier such that decay to the ground state will yield a rearrangement product.

Four rearrangement reactions and one elimination reaction will be discussed with activation barriers in the range 44.1–108.3 kcal/mol (Figure 6) which are suggestive of forbidden reactions. The orbital nature of the transition structure will be discussed in order to analyze how unfavorable interactions are minimized.

$\text{CH}_3\text{NO}_2 \rightarrow \text{CH}_3\text{ONO}$ . The concerted barrier for  $\text{CH}_3\text{NO}_2 \rightarrow \text{CH}_3\text{ONO}$  is calculated to be 73.5 kcal/mol. If the barrier to the radical pathway is assumed to be the same as the difference in energy between nitromethane and  $\text{CH}_3 + \text{NO}_2$ , the concerted barrier is 16.0 kcal/mol higher than the radical pathway.

(41) Williams, J. O.; Scarsdale, J. N.; Schafer, L.; Geise, H. J. *J. Mol. Struct.* **1981**, *76*, 11–28.

(42) Turner, P. H.; Cox, A. P. *J. Chem. Soc., Faraday Trans. 2*, **1978**, *74*, 533–559.

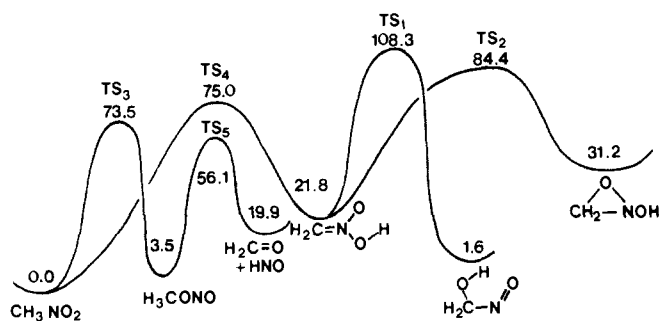


Figure 6. MERP (Minimum Energy Reaction Profile) for various rearrangements on the  $\text{CH}_3\text{NO}_2$  potential energy surface. Reported energies (kcal/mol) are relative to **1** at the MP2/6-31G\* + ZPC level.

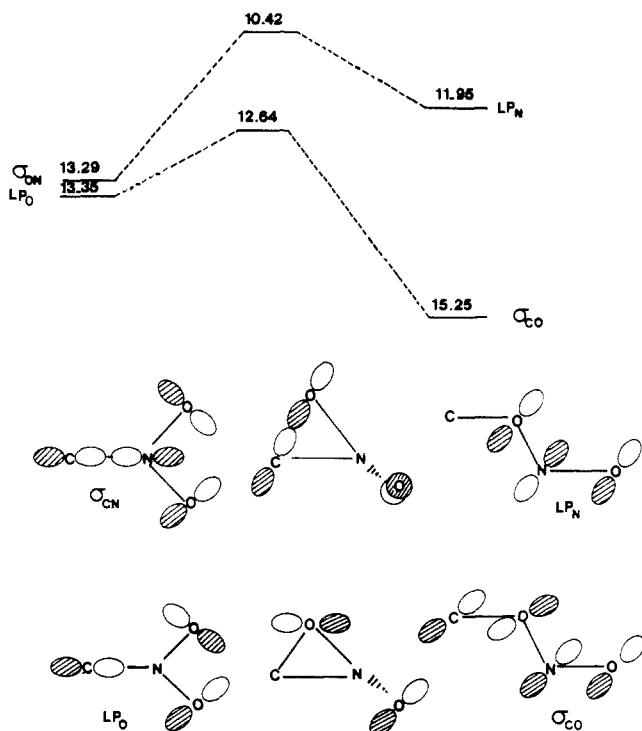


Figure 7. Diagram illustrating the transformation of  $\sigma_{\text{CN}}$  and oxygen lone pair orbitals in  $\text{CH}_3\text{NO}_2$  to the nitrogen lone pair and  $\sigma_{\text{CO}}$  orbitals in  $\text{CH}_3\text{ONO}$ . The high barrier can be attributed to the destabilizing effect of the  $\sigma_{\text{CN}}$  orbital in the transition structure.

The higher barrier can be attributed to the forbidden character of a 1,2 sigmatropic shift.<sup>43</sup> To illustrate which orbitals are destabilized in the reaction, the two highest  $\sigma$  orbitals (6-31G\*) of nitromethane (**1**), methyl nitrite (**6**), and the transition structure **21** for interconverting them are given in Figure 7. The  $\sigma_{\text{CN}}$  orbital, bonding in nitromethane, is antibonding in the transition structure and is destabilized by 66 kcal/mol (2.87 eV) which is close to the calculate barrier. Although many effects are responsible for a barrier, it is sufficient here to consider the destabilization of one orbital. The second  $\beta$  orbital is destabilized slightly (0.71 eV) at the transition state but is later stabilized by a large amount (2.61 eV) since this orbital becomes the C-O  $\sigma$  bond.

A qualitative potential surface of the  $\text{CH}_3\text{NO}_2 \rightarrow \text{CH}_3\text{ONO}$  rearrangement is provided in Figure 8. It might be reasoned that if the concerted pathway were higher than the radical pathway, then the former would collapse to the latter. This is not the case as the concerted transition structure ( $C_1$  symmetry) has one imaginary frequency. Higher in energy than the transition structure, a super saddle point must exist with two imaginary modes, one corresponding to rearrangement and the other to dissociation to radicals. It should be pointed out that in this study the transition

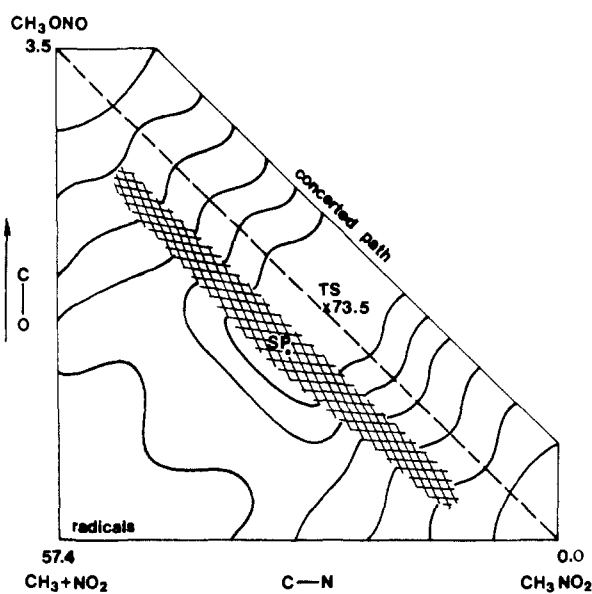


Figure 8. Qualitative illustration of the concerted rearrangement of  $\text{CH}_3\text{NO}_2 \rightarrow \text{CH}_3\text{ONO}$  (the transition structure is marked along diagonal), the radical pair formation (moving from bottom right to bottom left), and radical recombination (moving from bottom left to top left). A ridge (shaded) separates the two pathways such that the concerted transition structure, even though less stable than the radicals  $\text{CH}_3$  and  $\text{NO}_2$ , is still a genuine transition structure.

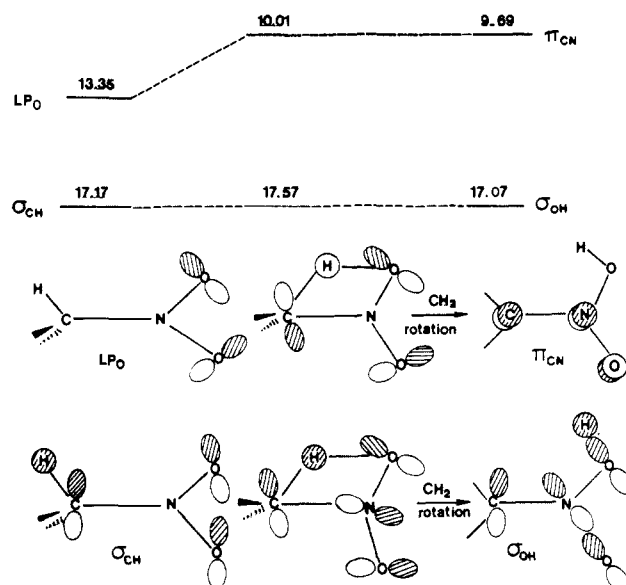


Figure 9. Diagram illustrating the transformation of the oxygen lone pair and  $\sigma_{\text{CH}}$  bond orbitals in  $\text{CH}_3\text{NO}_2$  to the  $\pi_{\text{CN}}$  and  $\sigma_{\text{OH}}$  bond orbitals in  $\text{CH}_2\text{N}(\text{O})\text{OH}$ . The oxygen lone pair transforms into a carbon lone pair if symmetry is maintained. When the  $\text{CH}_2$  group is allowed to rotate, the carbon lone pair forms the C=N bond.

structure and vibrational frequencies were calculated at the HF/6-31G\* level which cannot correctly describe the dissociation process to radicals. It is possible that at a higher level of theory or using a multiconfigurational approach the surface would be altered sufficiently to make the super saddle point more stable than the transition structure thereby eliminating the concerted pathway.

$\text{CH}_3\text{NO}_2 \rightarrow \text{H}_2\text{C}=\text{N}(\text{O})\text{OH}$ . The suprafacial 1,3 sigmatropic rearrangement of hydrogen is thermally forbidden.<sup>43</sup> An alternate route (albeit also of high energy) is the transfer of the hydrogen to a  $\sigma$  orbital rather than a  $\pi$  orbital. Such a transfer involves the smooth transformation of one orbital from  $\sigma_{\text{CH}}$  in nitromethane to  $\sigma_{\text{OH}}$  in  $\text{CH}_2=\text{N}(\text{O})\text{OH}$  (Figure 9). The high barrier is associated with an oxygen lone pair orbital which is strong antibonding in the transition structure. The oxygen lone pair is

(43) Lehr, R. E.; Marchand, A. P. *Orbital Symmetry: A Problem-Solving Approach*; Academic Press: New York, 1972.

destabilized by 77 kcal/mol (3.34 eV) in the transition structure which is nearly the same as the barrier height (75.0 kcal/mol).

Comparing the barrier height for the hydrogen transfer for **22** with the relative energy of CH<sub>2</sub>NO<sub>2</sub> + H for **26**, the concerted mechanism is 16.9 kcal/mol lower in energy. When the vibrational frequencies were calculated at the 6-31G\* level, two imaginary frequencies were obtained (1747i cm<sup>-1</sup> and 189i cm<sup>-1</sup>). The smaller imaginary frequency (indicating a CH<sub>2</sub> twisting motion) was absent in the 3-21G vibrational frequencies. In contrast to the 3-21G level, the 6-31G\* level predicts a favorable rotation in **22**, allowing the interaction of the HOMO (carbon lone pair) and the LUMO (nitrogen lone pair). The transition structure at the 6-31G\* level with one imaginary mode was not located.

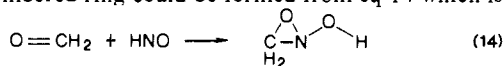
$\text{H}_2\text{C}=\text{N}(\text{O})\text{OH} \rightarrow \text{CH}_2\text{ONO}\text{H}$  and  $\text{H}_2\text{C}=\text{N}(\text{O})\text{OH} \rightarrow \text{CH}_2(\text{OH})\text{NO}$ . Two products can be obtained from **8** depending on whether the hydroxyl group migrates to form nitrosomethanol or the oxygen bends to carbon, forming the three-membered ring, *N*-hydroxyoxaziridine.

The electronic rearrangement necessary for each reaction can be best visualized by first rotating the CH<sub>2</sub> group perpendicular to the ONOH fragment. Two zwitterionic states should be close in energy as well as a biradical state. As the reaction proceeds and the plane of symmetry is lost, the three states will mix. The lower energy state will become the zwitterionic state with a formal positive charge on carbon. Movement of oxygen to form the three-membered ring will allow interaction of a lone pair on oxygen with the empty p orbital on carbon forming a  $\sigma$  C–O bond; migration of the hydroxyl group will allow the lone pair on oxygen to form a  $\sigma$  C–O bond, and at the same time, the  $\sigma$  N–O bond is transformed into a lone pair. The transition structure can be viewed as a thermally allowed 1,2 sigmatropic shift in a carbonium ion with inversion. Since the migrating or moving groups are hydroxyl and N=O, inversion or retention will not lead to different products.

A lower energy solution of the rotational transition state **10** is obtained with the zwitterionic configuration C<sup>-</sup> – N<sup>+</sup> occupied rather than C<sup>+</sup> – N<sup>-</sup>; however, as either the hydroxyl group migrates or the N=O group moves, the occupied orbitals on oxygen will decrease the contribution from C<sup>-</sup> – N<sup>+</sup> and increase the contribution from O<sup>+</sup> – N<sup>-</sup>. The biradical solution (UHF/6-31G\*) obtained by using the geometry of **10** is 11.0 kcal/mol more stable than the solution with the C<sup>-</sup> – N<sup>+</sup> configuration occupied. Correlation however reverses the stability and leads to a biradical solution 24.9 kcal/mol higher in energy. The rotational barrier is predicted to be 69.0 kcal/mol (**10** – **8**) at the MP2/6-31G\* + ZPC level.

Using the rotational transition structure as a reference, the migration of a hydroxyl group or movement of the N=O group becomes facile. The barrier for hydroxyl migration becomes 17.5 kcal/mol (**19** – **10**), while for N=O movement (forming a three-membered ring) a negative barrier results (-6.4 kcal/mol, **20** – **10**) indicating a spontaneous reaction for the hypothetical situation. The low barriers result from the favorable interaction of an occupied orbital on oxygen with an unoccupied orbital on carbon. The barriers from the lowest conformation of H<sub>2</sub>C=N(O)OH to nitrosomethanol and *N*-hydroxyoxaziridine are, of course, much higher (86.5 and 62.6 kcal/mol, respectively). Therefore, it is unlikely that either is formed in a concerted reaction.

*N*-hydroxyoxaziridine (**18**) has not been proposed in either the photolysis or pyrolysis of nitromethane or methyl nitrite.<sup>44</sup> The thermal barrier of 62.6 kcal/mol is still too high to be observed. The three-membered ring could be formed from eq 14 which is



calculated to be 11.3 kcal/mol endothermic. If the reverse barrier were not too small, it should be possible to observe  $\text{CH}_2\text{ONO}\text{H}$ .

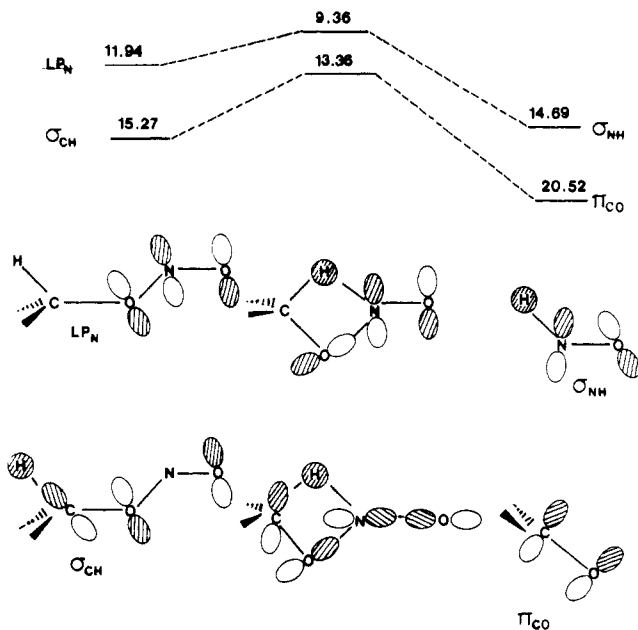


Figure 10. Diagram illustrating the transformation of the nitrogen lone pair and  $\sigma_{\text{CH}}$  orbitals in CH<sub>3</sub>ONO to the  $\sigma_{\text{NH}}$  of nitroxy and  $\pi_{\text{CO}}$  bond of formaldehyde. The orbital phases and energies are obtained from the C<sub>s</sub> stationary structure which is 8.5 kcal/mol higher than the true transition structure **23**.

In the photolysis of nitromethane, shifted peaks in the IR have been attributed to the hydrogen bond complex, CH<sub>2</sub>O...HNO.<sup>10,11</sup> It may be possible to codeposit the two species on an inert matrix and observe the three membered rings by irradiating at the HN stretching frequency.

$\text{CH}_3\text{ONO} \rightarrow \text{O}=\text{CH}_2 + \text{HNO}$ . It has been suggested<sup>1</sup> that methyl nitrite (**6**) might decompose by an intramolecular elimination to formaldehyde plus nitroxy (**25**) rather than to methoxy radical and nitric oxide (**27**). Dewar has recently reported<sup>33</sup> MINDO/3 calculations which predict an enthalpic barrier of 32.4 kcal/mol for this reaction (eq 12) which is lower than the barrier for N–O bond rupture. Taking into account a less favorable frequency factor for elimination, Dewar finds the two pathways competitive at 500 °C.

The transition structure for elimination found here (Figure 1, **23**) seems to indicate a reaction much closer to an elimination/abstraction reaction than the concerted reaction found by Dewar. The breaking N–O bond is much longer (2.016 Å, 6-31G\*; 1.289 Å, MINDO/3). The barrier at the MP2/6-31G\* + ZPC level is 44.1 kcal/mol which is 2.6 kcal/mol higher than the calculated enthalpy of CH<sub>2</sub>O + NO. One must therefore conclude that the elimination pathway is probably not competitive with N–O bond cleavage in CH<sub>3</sub>ONO.

The high barrier results from the destabilization of two orbitals in the transition structure. The nitrogen lone pair orbital is transformed into the NH  $\sigma$  bond of nitroxy while a CH  $\sigma$  bond is transformed into the C=O bond of formaldehyde (Figure 10).

#### Reaction Enthalpies of Fragmentation Reactions

No barriers to fragmentation were calculated due to the strong multiconfigurational nature of the reaction path. The energies of radical products were calculated however and compared with the CH<sub>3</sub>NO<sub>2</sub> surface in Tables I and II. The calculated relative energies at the MP2/6-31G\* + ZPC level are in good agreement with the experimental heats of formation at 298 K relative to the heat of formation of CH<sub>3</sub>NO<sub>2</sub>.

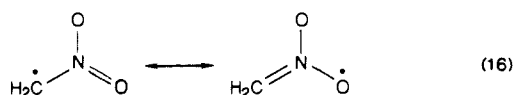
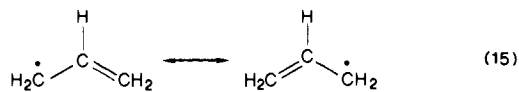
The bond energies indicated in eq 2 and 5 are very well reproduced. The C–N bond in CH<sub>3</sub>NO<sub>2</sub> is calculated to be 57.4 kcal/mol compared to the observed<sup>1</sup> bond energy of 58–60 kcal/mol. The terminal N–O bond energy in CH<sub>3</sub>ONO is also well reproduced (calcd 41.5; experimental<sup>1</sup> 39–41 kcal/mol) at the highest level despite a poor description of NO(<sup>2</sup>II) at the 6-31G\* level (due to a single configurational approach) which

(44) For a theoretical study of related three-membered rings, see: Popinger, D.; Radom, L.; Pople, J. A. *J. Am. Chem. Soc.* **1977**, *99*, 7806–7816.



leads to a large underestimation of the bond energy at that level.

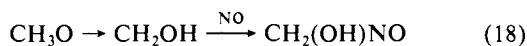
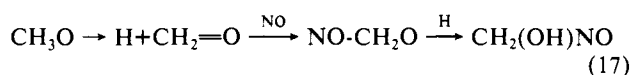
A significant disagreement exists between the calculated and experimental bond dissociation energy (BDE) of C–H in nitromethane. The calculated BDE of CH in nitromethane is similar to the BDE for the central CH bond in propene (91.9 and 88 kcal/mol, respectively). Compared to the standard C–H BDE (99 kcal/mol),<sup>45</sup> the CH bond in both propene and nitromethane are expected to be weaker due to resonance stabilization of the radical (eq 15 and 16).



The experimental C–H BDE of nitromethane (107.5 kcal/mol) which is based upon an estimated  $\Delta H_f$  for  $\text{CH}_2\text{NO}_2$ ,<sup>46</sup> is even higher than the BDE in  $\text{CH}_4$  (104.3 kcal/mol) for which no resonance stabilization is expected. The calculated BDE for  $\text{CH}_4 \rightarrow \text{CH}_3 + \text{H}$  at the level of theory employed here is 93.5 kcal/mol which is an underestimation of the BDE by 10.8 kcal/mol. If this error is transferrable to  $\text{CH}_3\text{NO}_2$ , the C–H BDE in this molecule would be 102.7 kcal/mol which is less than the experimental value but still unreasonably high. All calculations refer to the  $^2\text{B}_1$  state of  $\text{CH}_2\text{NO}_2$  which is the most stable state at the MP3/6-31G level.<sup>47</sup> However, at the MCSCF/6-31G + CI level a planar  $^2\text{A}''$  state was determined to be 14.6 kcal/mol more stable than the  $^2\text{B}_1$  state.<sup>47</sup> If this difference is applied to the estimated C–H BDE of nitromethane (91.9 + 10.8), the value decreases to 88.1 kcal/mol.

The nitromethyl radical may be an important intermediate in the formation of  $\text{H}_2\text{C}=\text{N}(\text{O})\text{OH}$  as shown in steps 8 and 9. The methyl radical should be formed readily in the photolysis or pyrolysis of  $\text{CH}_3\text{NO}_2$ . In step 8, the methyl radical can extract a hydrogen from another molecule of  $\text{CH}_3\text{NO}_2$  to form the nitromethyl radical in a reaction predicted to be exothermic by 1.6 kcal/mol. Step 9, the extraction of a hydrogen by an oxygen of  $\text{CH}_2\text{NO}_2$  to form  $\text{H}_2\text{C}=\text{N}(\text{O})\text{OH}$ , is predicted to be endothermic by 1.6 kcal/mol. The dominant configuration of the  $^2\text{B}_1$  state is an unpaired electron perpendicular to the molecular plane. However, due to other contributing configurations, the oxygen may compete with carbon for hydrogen abstraction.

The observed formation of nitrosomethanol in the pyrolysis of methyl nitrite cannot be due to a concerted rearrangement pathway since barrier heights are too high to be viable. Two possible radical pathways are given below. Since the methoxide radical,  $\text{CH}_3\text{O}$ ,



should be present from the cleavage of the weak N–O bond in  $\text{CH}_3\text{ONO}$ , an initial step might be the fission of a C–H bond to form  $\text{CH}_2=\text{O} + \text{H}$  which is predicted to be 19.6 kcal/mol (experimental 22.6 kcal/mol) exothermic or in a bimolecular step, hydrogen could be extracted from  $\text{CH}_3\text{O}$  by NO (eq 6) which is predicted to be 25.1 kcal/mol (experimental 22.6 kcal/mol) exothermic. The addition of NO to formaldehyde followed by abstraction of hydrogen by oxygen would then yield nitrosomethanol (eq 17). Alternatively, the methoxy radical,  $\text{CH}_3\text{O}$ , could rearrange to the hydroxymethyl radical,  $\text{CH}_2\text{OH}$  (eq 18).

The reaction has been calculated to have a barrier of 36.0 kcal/mol and to be endothermic 5.0 kcal/mol.<sup>48</sup> Subsequent addition of NO to the carbon of the hydroxymethyl radical would then also yield nitrosomethanol.

**Additivity Approximation.** The additivity approximation was tested for structures 1–23 by comparing relative energies at the [MP2/6-31G\*] level of theory with the full MP2/6-31G\* calculations (Table II). Ironically a better estimate of relative energies at the MP2/6-31G\* level is obtained by using the MP2/6-31G relative energies alone. Compounds containing nitro groups are known to have two configurations which mix strongly in the ground state.<sup>25–27</sup> Also, the dominance of the second configuration is sensitive to the computational level.<sup>26</sup> In this situation, additivity of polarization and correlation effects is not expected to be accurate because adding polarization functions not only increases the angular flexibility of the basis set but also changes the contribution of important low lying configurations. The correlation contribution at the lower level (6-31G) will not be a good indication of the contribution at the higher level (6-31G\*). To summarize, when the HOMO–LUMO gap is small or when additional configurations become important, additivity will not be accurate.

The relative energy of the three-membered ring 18 is not well represented at either the MP2/6-31G or [MP2/6-31G\*] level compared to the full MP2/6-31G\* calculation. The relative errors are 11.8 and 9.5 kcal/mol, respectively (Table II). The additivity results may be inaccurate due to the explanation given above, while the MP2/6-31G result does not include d orbitals on carbon, nitrogen, or oxygen, which may be important in a strained three-membered ring such as 18.

## Conclusion

Several concerted rearrangement pathways on the  $\text{CH}_3\text{NO}_2$  surface have been explored. The reactions all involve high energy barriers and are not expected to be competitive with free radical mechanisms. The conformational surface has been studied for nitromethane, methyl nitrite, *aci*-nitromethane, and nitrosomethanol. Agreement between theory and experiment is very good for methyl nitrite, lending confidence that the results for *aci*-nitromethane and nitrosomethanol may aid in structural studies. Two misleading stationary points of  $C_1$  symmetry were located on the nitrosomethanol conformational surface which disappeared after inclusion of correlation.

The origin of the high barriers to concerted reactions of nitromethane and *aci*-methyl nitrite can be attributed to a strongly antibonding interaction between a lone pair on oxygen and the migrating group (methyl group or hydrogen). An equivalent interpretation is the four electron-two orbital destabilizing interaction. The reaction,  $\text{R}_2\text{B}-\text{NO}_2 \rightarrow \text{R}_2\text{B}-\text{ONO}$ , which has been predicted<sup>33</sup> to be facile, would be an example of a two electron-two orbital stabilizing interaction.

The migration of a hydroxyl group or N=O movement forming a three-membered ring in *aci*-nitromethane can be viewed as an allowed thermal reaction starting from the appropriate electronic state of the rotational transition structure. The occupied orbital of the migrating group can then favorably interact with the empty orbital on carbon. Reactions from the planar structure of *aci*-nitromethane are unlikely due to the large amount of energy required to reach the rotational transition structure (69.0 kcal/mol).

It is hoped that the present study has provided a foundation for this complicated, yet important, potential energy surface.

**Acknowledgment.** Computer time for this study was donated by the Auburn University Computer Center.

**Registry No.** 1, 75-52-5; 3, 624-91-9; 8, 4167-98-0; 11, 86146-57-8; 18, 103368-30-5.

(45) Sanderson, R. T. *Chemical Bonds and Bond Energy*, 2nd ed.; Academic Press: New York, 1976.

(46) Knobel, Yu. K.; Miroshnichenko, E. A.; Lebedev, Yu. *Izv. Akad. Nauk. SSSR, Ser. Khim.* **1971**, 20, 425.

(47) McKee, M. L. *J. Chem. Phys.* **1984**, 81, 3580–3587.

(48) Saeko, S.; Radom, L.; Schaefer, H. F. *J. Chem. Phys.* **1983**, 78, 845–853.